Cell PRESS
Immunity
Article

Reversal of Autoimmunity by Boosting Memory-like Autoregulatory T Cells

Sue Tsai,[1,2,5] Afshin Shameli,[1,2,5] Jun Yamanouchi,[1,2] Xavier Clemente-Casares,[1,2] Jinguo Wang,[1,2] Pau Serra,[1,2] Yang Yang,[1,2,3] Zdravka Medarova,[4] Anna Moore,[4] and Pere Santamaria[1,2,*]
[1]Julia McFarlane Diabetes Research Centre, Department of Microbiology and Infectious Diseases
[2]Institute of Inflammation, Infection and Immunity
[3]Department of Biochemistry and Molecular Biology, Faculty of Medicine
The University of Calgary, 3330 Hospital Drive N.W., Calgary, AB T2N 4N1, Canada
[4]Department of Radiology, Molecular Imaging Laboratory, MGH/MIT/HMS Athinoula A. Martinos Center for Biomedical Imaging, Massachusetts General Hospital, Building 75, 13th Street, Charlestown, MA 02129, USA
[5]These authors contributed equally to this work
*Correspondence: psantama@ucalgary.ca
DOI 10.1016/j.immuni.2010.03.015

SUMMARY

Blunting autoreactivity without compromising immunity remains an elusive goal in the treatment of autoimmunity. We show that progression to autoimmune diabetes results in the conversion of naive low-avidity autoreactive CD8$^+$ T cells into memory-like autoregulatory cells that can be expanded in vivo with nanoparticles coated with disease-relevant peptide-major histocompatibility complexes (pMHC-NP). Treatment of NOD mice with monospecific pMHC-NPs expanded cognate autoregulatory T cells, suppressed the recruitment of noncognate specificities, prevented disease in prediabetic mice, and restored normoglycemia in diabetic animals. pMHC-NP therapy was inconsequential in mice engineered to bear an immune system unresponsive to the corresponding epitope, owing to absence of epitope-experienced autoregulatory T cells. pMHC-NP-expanded autoregulatory T cells suppressed local presentation of autoantigens in an interferon-γ-, indoleamine 2,3-dioxygenase-, and perforin-dependent manner. Nanoparticles coated with human diabetes-relevant pHLA complexes restored normoglycemia in a humanized model of diabetes. These observations expose a paradigm in the pathogenesis of autoimmunity amenable for therapeutic intervention.

INTRODUCTION

Spontaneous autoimmune disorders typically result from polyclonal immune responses against many antigens. Although non-antigen-specific, mAb-based immunosuppressive approaches have shown benefit in clinical trials (Kaufman and Herold, 2009), these strategies bear the inherent risk of compromising immunity to infections and cancer.

Type 1 diabetes (T1D) in both humans and nonobese diabetic (NOD) mice is a chronic autoimmune disease that results from destruction of pancreatic β cells by CD4$^+$ and CD8$^+$ T cells targeting many antigens (Lieberman and DiLorenzo, 2003; Tsai et al., 2008). A large fraction of the islet-associated CD8$^+$ cells in NOD mice recognize the mimotopes NRP-A7 and -V7 in the context of the MHC molecule K^d (Verdaguer et al., 1996, 1997; Anderson et al., 1999). These T cells are diabetogenic (Verdaguer et al., 1997), target a peptide from islet-specific glucose-6-phosphatase catalytic subunit-related protein (IGRP$_{206-214}$, similar to NRP-A7 and -V7) (Lieberman et al., 2003), and circulate in the blood, particularly as clinical disease nears (Trudeau et al., 2003). Another important feature of the diabetogenic CD8$^+$ response is that it involves recognition, by smaller T cell pools, of many other IGRP epitopes (Han et al., 2005a) and epitopes in other, even ubiquitous, autoantigens, such as dystrophia myotonica kinase (DMK) (Lieberman et al., 2004). The polyspecificity of this T cell response is compounded by the fact that individual specificities harbor clones engaging pMHC over a range of avidities, the strength of which correlates with pathogenic potential (Amrani et al., 2000).

This complexity is a barrier to the design of therapeutic strategies that selectively purge the immune system of autoreactivity without impairing systemic immunity. Soluble peptides can induce peptide-specific T cell tolerance (Aichele et al., 1994) but cannot blunt polyspecific autoimmune responses, unless they target key disease-triggering autoantigen(s) and are administered before other autoantigenic specificities become involved. Unfortunately, this situation only applies to the earliest stages of disease. For example, despite effectively deleting the IGRP$_{206-214}$-reactive CD8$^+$ pool, NRP-V7 therapy did not protect NOD mice from T1D because it fostered occupation of the voided intraislet "niche" by CD8$^+$ cells recognizing other epitopes (Han et al., 2005a). This suggested that therapeutic success might require deletion of multiple antigenic specificities. Because peptides are more tolerogenic when bound to MHC molecules on costimulation-impaired APCs than when used in solution (Miller et al., 1979), we envisioned that simultaneous delivery of several different T1D-relevant peptide-MHC (pMHC) complexes by nanoparticles (NPs) would enable the type of combinatorial autoantigen therapy needed to blunt T1D.

Unexpectedly, we found that monospecific pMHC-NP therapy was able to both blunt T1D progression in prediabetic mice and

restore normoglycemia in newly diagnosed diabetic animals. Most surprisingly, we found that pMHC-NP therapy functions by expanding, in an epitope-specific manner, a subset of antigen-experienced autoreactive $CD8^+$ cells that suppresses the activation and recruitment of noncognate specificities to islets. These memory-like "autoregulatory" $CD8^+$ cells arise spontaneously (during disease—prior to pMHC-NP therapy—and within different autoantigen-specific T cell pools) from nonpathogenic low-avidity clones and blunt the recruitment of other specificities by suppressing presentation of autoantigens in the pancreas-draining lymph nodes. Because these pools of protective antigen-experienced $CD8^+$ cells are not limited to specific epitopes or autoantigens and arise only in affected, but not healthy, individuals, NPs coated with any disease-relevant pMHC complex have the potential to become powerful vaccines capable of blunting and resolving polyclonal autoimmune responses in a disease-specific manner.

RESULTS

pMHC-NPs Blunt T1D while Expanding Cognate Low-Avidity Autoreactive T Cells

To ascertain if pMHC-NPs could delete cognate $CD8^+$ cells, we treated NRP-V7 ($IGRP_{206-214}$)-reactive 17.4α-8.3β-TCR-transgenic NOD mice (Verdaguer et al., 1997) with NRP-V7-K^d-NPs (Moore et al., 2004). The naive $CD8^+$ cells of these mice were gradually deleted, and those escaping deletion showed reduced recall proliferation in vitro (Figures S1A and S1B).

Since T1D in wild-type NOD mice involves many antigenic specificities, we reasoned that prevention of disease might require the use of pools of NPs coated with different pMHCs. Because ~40% of islet $CD8^+$ cells recognize epitopes from IGRP (Han et al., 2005a), we synthesized pMHC-coated NPs (pMHC-NP) targeting the six most prevalent pools of IGRP-specific $CD8^+$ cells. We treated young NOD mice (every 2 to 3 weeks) with a mixture of these six pMHC-NP types or with control NP (carrying biotin or a T1D-irrelevant pMHC [TUM-K^d]). Mice treated with the NP pool, unlike those receiving control NP, were 100% protected from T1D (data not shown). As an additional control, we used NRP-V7-K^d-NPs alone, which were expected to delete the entire $IGRP_{206-214}$-reactive pool *without* blunting T1D progression.

Unexpectedly, NRP-V7-K^d-NPs protected mice from T1D (Figure 1A), but not insulitis (Figure 1B). Most surprisingly, these mice had significantly *larger* pools of circulating and intra-islet NRP-V7-K^d tetramer$^+$ $CD8^+$ cells versus control NP-treated or untreated animals ($p < 0.05$; Figures 1C and 1D). Similar results were obtained with NP coated with $IGRP_{206-214}$-K^d (Figure 1A). Comparison of mice that had progressed to diabetes versus those that did not suggested an association between the anti-T1D effect of NRP-V7-K^d-NP and expansion of cognate $CD8^+$ cells (Figure 1E). Furthermore, these T cell-expanding and anti-T1D effects were dose dependent (Figures S1C and S1D) and cumulative (Figure S1E). Additional studies showed that these NPs are taken up by cognate T cells without accumulating in $CD11b^+$, $CD11c^+$, or B cells (Figures S1F and S1G).

Because the islets of young prediabetic NOD mice are enriched for low-avidity autoreactive $CD8^+$ clones (Amrani et al., 2000) and these clones appear to slow down the diabetogenic process (Amrani et al., 2000; Han et al., 2005a), we asked if the cells that had expanded in response to pMHC-NP therapy belonged to this low-avidity subset. Indeed, the intraislet NRP-V7-K^d tetramer$^+$ $CD8^+$ cells of NRP-V7-K^d-NP-treated mice bound pMHC with significantly lower avidity (>K_d) than those of control mice ($p = 0.01$;Figure 1F). Furthermore, treatment with NRP-V7-K^d-NPs induced changes in the TCRα repertoire of islet-associated NRP-V7-K^d-tetramer$^+$ cells, consistent with enrichment for low-avidity clones, expressing Vα17.6-Jα42 chains using noncanonical CDR3α sequences (other than MRD-E) (Figure 1G).

We next wondered if the T cell-expanding and anti-T1D effects of pMHC-NP were a peculiarity of NRP-V7-K^d or $IGRP_{206-214}$-K^d. We treated NOD mice with NP coated with D^b presenting a mimotope for $DMK_{138-146}$ (MimA2), which is targeted by a much smaller subset of $CD8^+$ cells (Lieberman et al., 2004). MimA2-D^b-NPs expanded the circulating and intraislet MimA2-D^{b+} $CD8^+$ pools several fold, in this case from virtually undetectable levels (Figures 1H and 1I), and afforded T1D protection (Figure 1J). Comparative measurements of avidity were not possible here because the size of the MimA2-reactive subset in islets of untreated NOD mice is too small (Figure 1I). Importantly, T cell expansion by these two different types of pMHC-NP was antigen specific (Figures S1H–S1J).

We then asked if enhanced recruitment of pMHC-NP-expanded $CD8^+$ cells impaired the recruitment of other autoreactive $CD8^+$ cells. We compared the responsiveness of the islet-derived $CD8^+$ cells of mice treated with control and NRP-V7-K^d- or MimA2-D^b-NP to a panel of 76 different IGRP epitopes (Han et al., 2005a). Islet-associated T cells were short-term expanded using an approach that does not significantly alter the relative distribution of autoreactive specificities as found in uncultured islets (Figures S1K and S1L). As shown in Figure 1K, pMHC-NP-treated mice recruited substantially fewer $CD8^+$ specificities than control mice. Thus, NPs coated with T1D-relevant pMHCs blunt the recruitment of noncognate T cell specificities and T1D by expanding cognate low-avidity autoreactive $CD8^+$ T cells.

pMHC-NP Therapy Restores Normoglycemia in Diabetic NOD Mice

To investigate if monospecific pMHC-NP therapy could restore normoglycemia in diabetic mice, we randomized newly diabetic animals into treatment with TUM-K^d-NP (control), NRP-V7-K^d-NP, or MimA2-D^b-NP. All mice received two weekly doses of NP and were monitored twice a week for blood glucose. An additional cohort was treated with NRP-V7-K^d tetramers, using amounts of pMHC similar to those given when coated onto NPs. Treatment with CD3 mAb was used as a positive control. Unlike mice treated with TUM-K^d-NP or pMHC tetramers, most (>75%) NRP-V7-K^d-NP- and MimA2-D^b-NP-treated mice became normoglycemic (Figures 2A and 2B and Figure S2D) and displayed large increases in the peripheral frequency of tetramer$^+$ $CD8^+$ cells (Figures S2A and S2B). No differences in the peripheral frequency $FoxP3^+CD4^+$ Treg cells were observed (Figure S2C). Four of six mice treated with CD3 mAb also became normoglycemic (Figure S2D). Thus, the NP component of pMHC-NPs is essential, and the effectiveness of the pMHC-NP approach is comparable to that of CD3 mAb. Histopathological

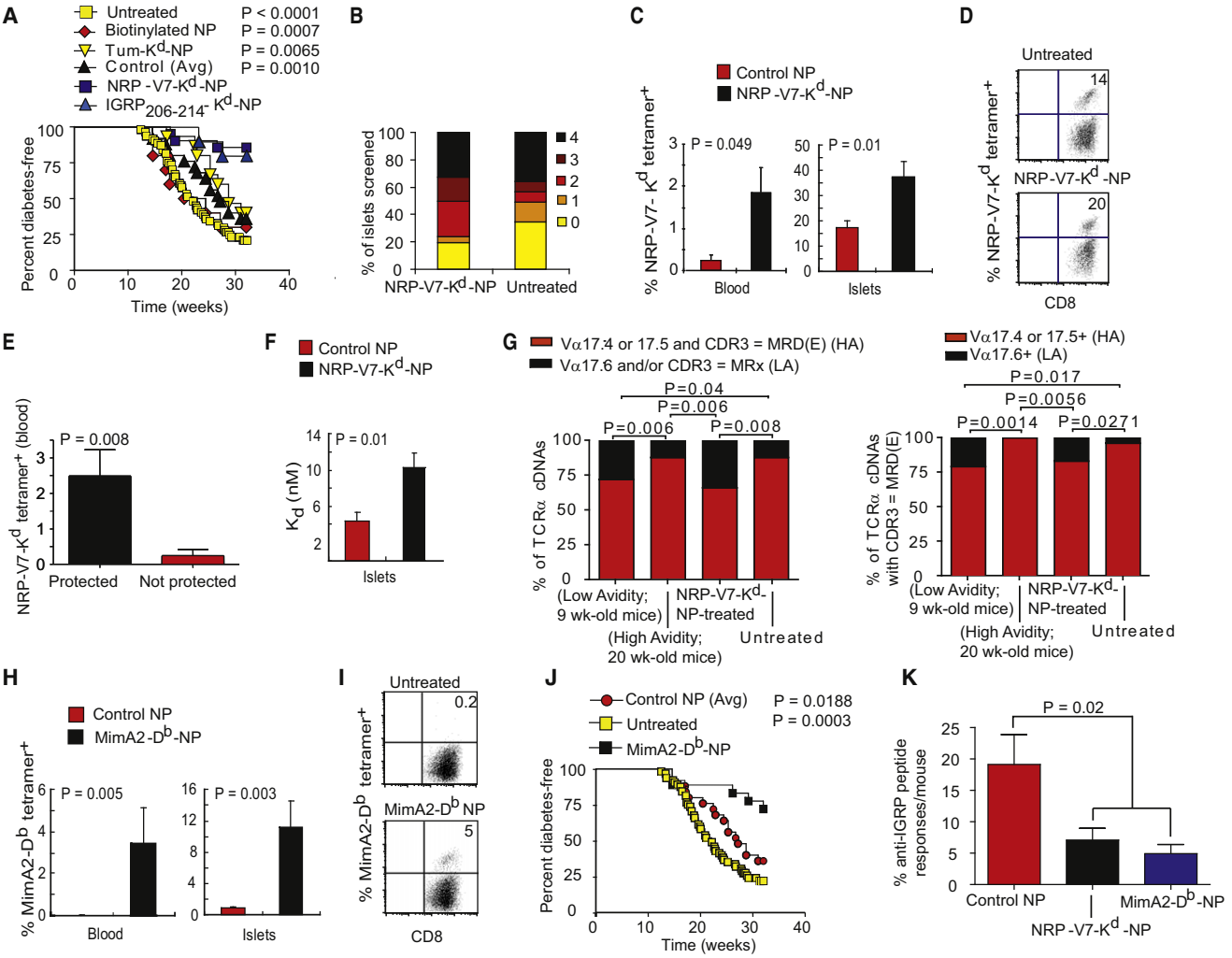

Figure 1. pMHC-NPs Expand Low-Avidity Autoreactive CD8$^+$ Cells and Protect NOD Mice from Diabetes

(A) NOD mice were left untreated (n = 65) or injected i.v. with 7.5 μg of NRP-V7-K^d-NP (n = 21) IGRP$_{206-214}$-K^d-NP (n = 10) or control NP (TUM-K^d- [n = 15] or biotin-coated NP [n = 10]) at 4, 6, and 8 weeks and every 3 weeks until the 32nd week. p values are versus the NRP-V7-K^d-NP group.

(B) Insulitis scores in nondiabetic mice at 32 weeks (pMHC-NP-treated, n = 4; untreated, n = 3).

(C) NRP-V7-K^d-NP expanded NRP-V7-K^d tetramer$^+$ CD8$^+$ cells in blood (n = 14) and enhanced their recruitment to islets (n = 11) versus control-NP-treated mice (n = 4 and 21, for blood and islets, respectively). Data correspond to percent tetramer$^+$ cells (± SEM) within the CD8$^+$ gate. Islet-associated CD8$^+$ cells were from individual mice.

(D) Representative tetramer stains for islet-derived CD8$^+$ cells of NRP-V7-K^d-NP-treated mice.

(E) Only protected, but not diabetic, NRP-V7-K^d-NP-treated NOD mice had expanded pools of NRP-V7-K^d-tetramer$^+$ cells in blood (n = 10 and 4, respectively).

(F) The islet-associated CD8$^+$ cells of NRP-V7-K^d-NP-treated mice (n = 5) bound pMHC with lower avidity than those from untreated age-matched NOD mice (n = 11).

(G) TCRα repertoire of NRP-V7-K^d-tetramer$^+$ cells from untreated 9- and 20-week-old NOD mice and 15 week-old NOD mice that had either been treated for 5 weeks with NRP-V7-K^d-NP starting at 10 weeks of age or left untreated. Data correspond to 57-58 cDNA clones/group from two independent experiments. HA, high-avidity; LA, low-avidity, as defined by comparing the TCR repertoires of the LA pools of 9-week-old NOD mice and the HA pools of 20-week-old NOD mice (Han et al., 2005b). In MRx, x corresponds to any amino acid other than D or E.

(H) MimA2-D^b-NP expand MimA2-D^b tetramer$^+$ CD8$^+$ cells in blood (n = 11) and islets (n = 13) versus controls (n = 4 and 3). Data correspond to nondiabetic mice at the end of follow-up.

(I) Representative tetramer stains for islet-derived CD8$^+$ cells of untreated and MimA2-D^b-NP-treated mice.

(J) Disease curves for MimA2-D^b-NP-treated (n = 18) versus control groups (control-NP, n = 25; untreated, n = 65).

(K) Islet-associated CD8$^+$ cells from control-NP-treated (n = 9), NRP-V7-K^d-NP-treated (n = 5), and MimA2-D^b-NP-treated (n = 4) mice were assayed for IFNγ production in response to splenocytes pulsed with each of 76 different IGRP epitopes or the negative control TUM, and the number of positive responses (>50 pg/ml) was counted. Panel displays the percent of peptides that elicited positive responses in CD8$^+$ cells from individual mice (mean ± SEM).

See also Figure S1.

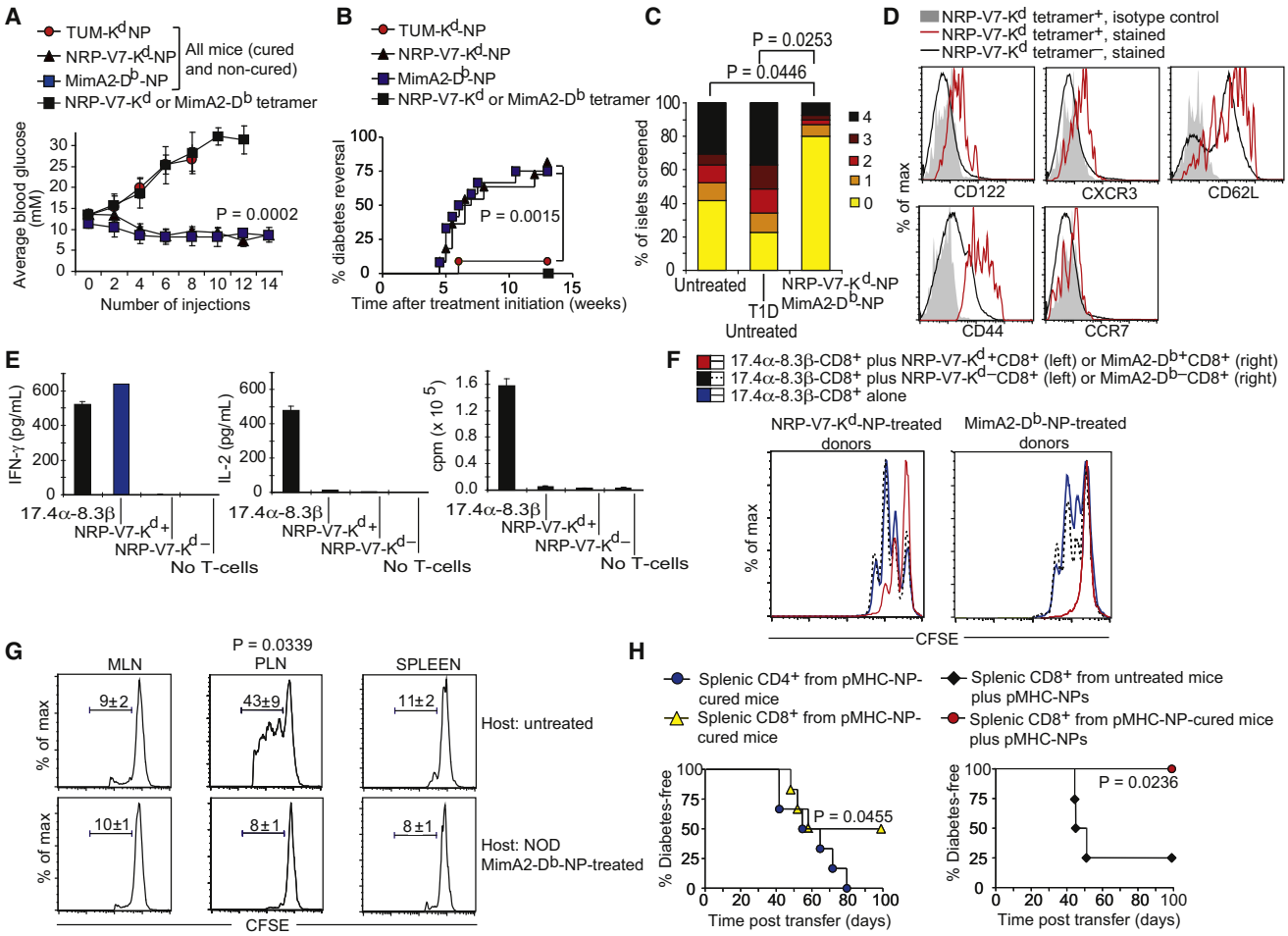

Figure 2. NRP-V7-K^d- and MimA2-D^b-NP Restore Normoglycemia in Diabetic NOD Mice by Expanding Memory-like Antidiabetogenic CD8$^+$ T Cells

(A) Average blood glucose/group (includes diabetic and nondiabetic mice; the average nonfasting blood glucose levels in the "cured" mice were <8 mM and similar to nondiabetic untreated mice). NOD mice with > 11 mM of blood glucose were treated with NRP-V7-K^d tetramers (n = 5), TUM-K^d-NP (n = 9), NRP-V7-K^d-NP (n = 11), or MimA2-D^b-NP (n = 11) (until normoglycemic for 4 weeks).

(B) Disease incidence curves.

(C) Insulitis scores in nondiabetic untreated 50-week-old mice (n = 6) at the onset of diabetes prior to the initiation of treatment (n = 3; 16–22 weeks) and after restoration of normoglycemia (50 weeks; n = 5). The scores were 1.93 ± 0.39, 2.42 ± 0.12, and 0.64 ± 0.16, respectively.

(D) Representative flow cytometry profiles of tetramer$^+$ and tetramer$^-$ CD8$^+$ cells from NRP-V7-K^d-NP-treated mice.

(E) Sorted pMHC-NP-expanded tetramer$^+$ CD8$^+$ cells secrete IFN-γ but do not produce IL-2 or proliferate in response to peptide-pulsed DCs.

(F) In vitro suppression of 17.4α-8.3β-CD8$^+$ proliferation by pMHC-NP-expanded NRP-V7-K^d or MimA2-D^b tetramer$^+$CD8$^+$ cells (in response to NRP-V7- [left] or NRP-V7+MimA2-pulsed DCs [right]).

(G) Proliferation of CFSE-labeled 17.4α-8.3β-CD8$^+$ cells in the MLN, PLN, and spleen of untreated age-matched NOD mice or MimA2-D^b-NP-cured mice (at 35 weeks). Data correspond to five and three mice, respectively.

(H) Left: MimA2-D^b-NP-expanded CD8$^+$ cells from cured NOD mice (n = 6; 5 × 10^6 CD8$^+$ cells, containing < 5 × 10^4 MimA2-D^b tetramer$^+$ cells) suppress the adoptive transfer of diabetes by splenic T cells from prediabetic NOD mice into NOD.*scid* females compared to total CD4$^+$ cells (5 × 10^6) from cured donors (n = 6). Right: NRP-V7-K^d-NP treatment (twice/week) potentiates the transfer of protection by splenic CD8$^+$ cells from NRP-V7-K^d-NP-cured mice into T cell-reconstituted NOD.*scid* hosts (n = 3) but cannot induce protective activity in splenic CD8$^+$ T cells from untreated NOD donors (n = 4).

See also Figure S2.

analyses of cured mice at 50 weeks revealed increased percentages of noninfiltrated islets, compared to age-matched nondiabetic untreated mice and mice immediately before treatment (Figure 2C and Figure S2E). Withdrawal of therapy after 4 weeks of normoglycemia resulted in a progressive decline in the size of the circulating tetramer$^+$ pool (Figure S2B) and a 40%–50% recurrence rate within 20 weeks (Figures S2D and S2F), suggesting that the protective effects of pMHC-NP wane without boosting. Weight assessments, intraperitoneal glucose tolerance tests, and serum insulin measurements confirmed that pMHC-NP therapy restored the insulin secretory capacity of the pancreas (Figures S2G–S2J). Thus, when initiated shortly after onset of hyperglycemia, pMHC-NP therapy protects β cells from further attack, enabling functional recovery.

The pMHC-NP-Expanded Low-Avidity CD8$^+$ Cells Are Memory-like and Regulatory

The tetramer$^+$ cells of NRP-V7-K^d- and MimA2-D^b-NP-treated mice were FoxP3$^-$, CD69$^-$, and CD25$^-$ (data not shown) but enriched for cells expressing the memory markers CD44 and CD122. These memory-like CD44^{hi}CD122$^+$CD8$^+$ cells were CCR7$^-$, CXCR3$^+$, and CD62L^{hi} (Figure 2D), a phenotype different from that of classical central and effector memory T cells (Sallusto et al., 2004) or the CD122$^+$CD8$^+$ Treg subset described in healthy strains (Endharti et al., 2005). Like conventional memory T cells, these CD8$^+$ cells produced high amounts of IFN-γ in response to antigen-pulsed DCs (Figure 2E). However, unlike naive and conventional memory CD8$^+$ cells, they neither secreted IL-2 nor proliferated (Figure 2E).

In vitro, these pMHC-NP-expanded T cells suppressed the proliferation of CFSE-labeled 17.4α-8.3β-CD8$^+$ cells in response to peptide-pulsed DCs (Figure 2F and Figure S2K). Suppression was antigen nonspecific because the MimA2-D^b tetramer$^+$ CD8$^+$ cells of MimA2-D^b-NP-treated mice could suppress the proliferation of CFSE-labeled NRP-V7-K^d-specific 17.4α-8.3β-CD8$^+$ cells to DCs pulsed with both MimA2 plus NRP-V7 (Figure 2F). These pMHC-expanded cells also had regulatory activity in vivo. Thus, the PLNs of MimA2-D^b-NP-treated NOD mice, unlike those from untreated age-matched controls, could not support the proliferation of naive CFSE-labeled 17.4α-8.3β-CD8$^+$ cells (Figure 2G). Furthermore, splenic CD8$^+$ (but not CD4$^+$) cells from pMHC-NP-cured mice inhibited the transfer of diabetes by wild-type NOD splenic T cells into NOD.*scid* recipients (Figure 2H). In addition, pMHC-NP treatment of the hosts enhanced the anti-T1D properties of CD8$^+$ cells from pMHC-cured mice without eliciting antidiabetogenic activity in CD8$^+$ cells from untreated NOD donors (Figure 2H). Thus, the CD8$^+$ T cells that expand in response to pMHC-NP therapy are memory like and regulatory.

pMHC-NPs Operate via Disease-Generated Autoregulatory CD8$^+$ Cells

As noted above, pMHC-NP therapy in TCR-TG and wild-type NOD mice yielded seemingly contradictory results: whereas pMHC-NP therapy deleted naive autoreactive CD8$^+$ cells in TCR-TG mice, it expanded low avidity memory-like autoregulatory CD8$^+$ cells in NOD mice. Four observations prompted us to suspect that past autoantigen-experience (i.e., memory) underlie these differences in responsiveness to pMHC-NP. First, unlike naive T cells, memory T cells can expand in response to TCR ligation without costimulation (Bachmann et al., 1999). Second, treatment of NOD mice with TUM-K^d-NP (a T1D-irrelevant pMHC complex) did not expand TUM-reactive CD8$^+$ cells (Figure S3A). Third, the peripheral frequencies of tetramer$^+$CD8$^+$ cells in NRP-V7-K^d-NP-treated B10.*H2*^{g7} mice, which do not develop insulitis and thus should not contain NRP-V7-K^d-experienced CD8$^+$ clones, were similar to those seen in untreated age-matched littermates (Figure S3B). And fourth, systemic expansion of NRP-V7-K^d-tetramer$^+$ CD8$^+$ cells in NRP-V7-K^d-NP-treated NOD mice was more effective when initiated at diabetes onset than in the prediabetic stage, presumably because the size of the expandable memory T cell pool increases with time (Figure S3C).

We thus sought to investigate the consequences of NRP-V7-K^d- and MimA2-D^b-NP treatment in a gene-targeted NOD strain expressing a mutant form of IGRP (encoded in *G6pc2*) in which the two TCR-contact residues of IGRP$_{206\text{-}214}$ (Amrani et al., 2001) are replaced with alanines (K209A and F213A) (Figure 3A). NOD.*G6pc2*$^{K209A\text{-}F213A}$ mice could not recruit peripheral IGRP$_{206\text{-}214}$-reactive T cells into islets and thus generate IGRP$_{206\text{-}214}$-experienced T cells (Figures 3B and 3C). As a result, treatment of 10-week-old NOD.*G6pc2*$^{K209A\text{-}F213A}$ mice with 10 doses of NRP-V7-K^d-NP over 5 weeks failed to expand NRP-V7-K^d-reactive CD8$^+$ cells (Figure 3B). Thus, pMHC-NPs only expand autoantigen-experienced CD8$^+$ cells. We then treated spontaneously hyperglycemic NOD.*G6pc2*$^{K209A\text{-}F213A}$ mice with NRP-V7-K^d- or MimA2-D^b-NP. Whereas MimA2-D^b-NP expanded the circulating MimA2-D^b-reactive CD8$^+$ pool (Figure 3D) and restored normoglycemia in five of six mice (Figure 3E and Figrue S3D), treatment with NRP-V7-K^d-NP neither expanded NRP-V7-K^d-reactive T cells (Figure 3D) nor restored normoglycemia in the five mice tested (Figure 3E and Figure S3D). Thus, pMHC-NPs afford diabetes resistance via disease-induced, autoantigen-experienced CD8$^+$ T cell pools.

"Memory" Autoregulatory Cells Arise from Low-Avidity Precursors

The data suggested that the autoantigen-experienced regulatory CD8$^+$ cells that expand in response to pMHC-NPs arise from low-avidity precursors. This hypothesis predicted that low-avidity autoreactive CD8$^+$ cells maturing in NOD mice *spontaneously* differentiate into memory-like autoregulatory T cells. To test this hypothesis, we cloned an NRP-V7-K^d-reactive TCR using the 8.3-TCRβ chain and a TCRα chain enriched in the low-avidity CD8$^+$ infiltrates of NRP-V7-K^d-NP-treated NOD mice (Vα17.6-MRD-Jα42) (Figure 1G). This TCR$\alpha\beta$ recognizes NRP-V7-K^d with ~10 times lower affinity (measured by surface plasmon resonance; L. Teyton and P.Santamaria, unpublished data) than the 17.4α-8.3β-TCR, which uses the same TCRβ but a slightly different TCRα (enriched in the high-avidity CD8$^+$ infiltrates of untreated controls [Vα17.4-MRD-Jα42]) (Figures 1G). We refer to these TCRs as 17.6α-8.3β (low-affinity) and 17.4α-8.3β (high-affinity), respectively.

We compared the developmental biology of these TCRs in TCR-TG NOD mice. Both fostered the development of peripheral CD8$^+$ repertoires dominated by functional IGRP$_{206\text{-}214}$-reactive CD8$^+$ cells, albeit with different efficiencies, as expected (Figures S4A–S4D and data not shown). However, whereas 17.4α-8.3β-TG mice developed accelerated T1D (versus wild-type NOD mice) (Verdaguer et al., 1997), 17.6α-8.3β-TG NOD mice were almost completely resistant to insulitis and T1D, even in mice unable to rearrange endogenous TCRα chains (Figures S4E–S4G) and despite harboring fewer CD4$^+$CD25$^+$ Treg cells (Figure S4H). The T1D resistance of 17.6α-8.3β-TG mice could not be explained by mere dilution of the endogenous diabetogenic T cell repertoire because NOD mice expressing a T1D-irrelevant TCR developed T1D like NOD mice (Figure S4I) (see also Serreze et al., 2001).

We next asked if the low- and high-avidity autoreactive CD8$^+$ cells maturing in 17.6α-8.3β- and 17.4α-8.3β-TG NOD mice, respectively, *spontaneously* differentiated into memory-like T cells. The peripheral tetramer$^+$ CD8$^+$ pool of 17.6α-8.3β- but not 17.4α-8.3β-TG mice, was enriched for CD44^{hi}CD122$^+$ cells, particularly in 17.6α-8.3β-NOD.*Tcra*$^{-/-}$ mice (Figures 4A

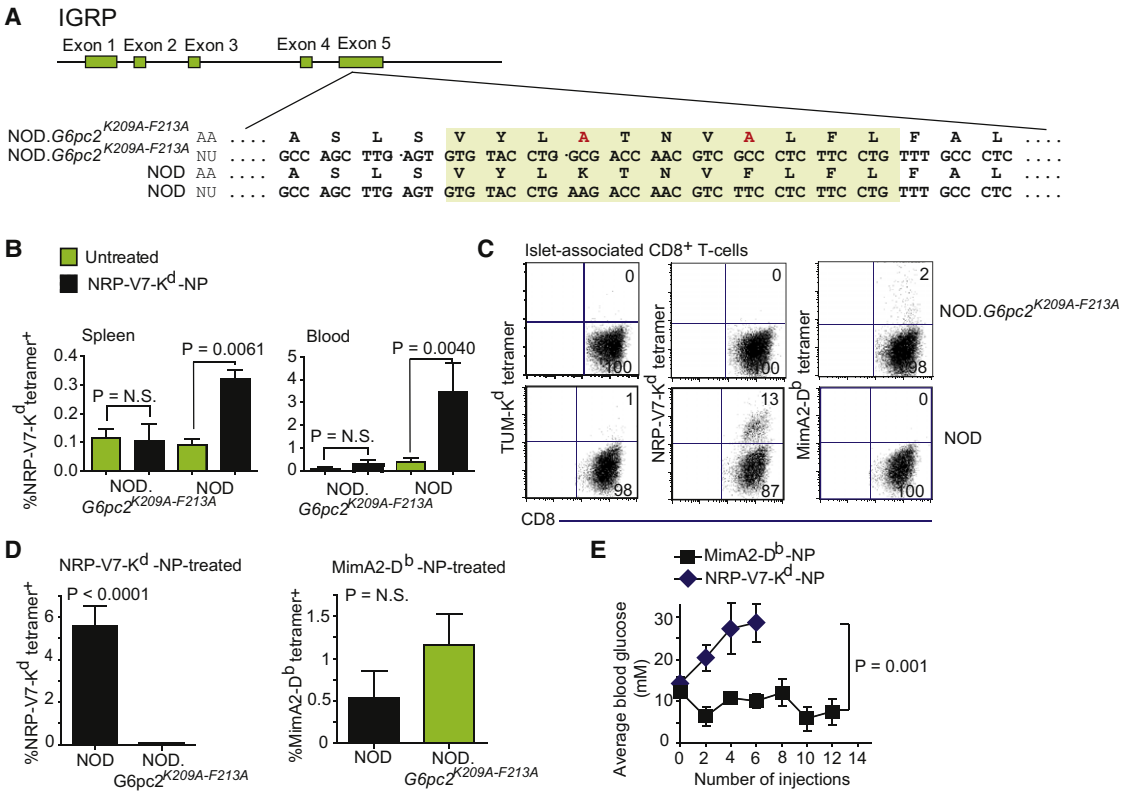

Figure 3. pMHC-NP Operate via Antigen-Experienced T Cells

(A) Schematic diagram comparing *G6pc2* (encoding IGRP) from NOD versus NOD.*G6pc2*$^{K209A-F213A}$ mice.

(B) Percentages of NRP-V7-K^d tetramer$^+$ CD8$^+$ cells in spleen and blood in untreated and NRP-V7-K^d-NP-treated NOD versus NOD.*G6pc2*$^{K209A-F213A}$ mice (n = 4–9/mouse type). Mice were treated twice/week with NRP-V7-K^d-NP from the 10th to the 15th week of age.

(C) Representative TUM-K^d, NRP-V7-K^d, and MimA2-D^b-tetramer-staining profiles of islet-associated CD8$^+$ cells in diabetic NOD versus NOD.*G6pc2*$^{K209A-F213A}$ mice.

(D) Percentages of circulating NRP-V7-K^d or MimA2-D^b-tetramer$^+$ CD8$^+$ cells in NRP-V7-K^d-NP- or MimA2-D^b-NP-treated NOD versus NOD.*G6pc2*$^{K209A-F213A}$ mice, respectively (n = 3–6 samples/mouse type/NP type).

(E) Average blood glucose amounts in NRP-V7-K^d-NP- or MimA2-D^b-NP-treated NOD.*G6pc2*$^{K209A-F213A}$ mice.

See also Figure S3.

and 4B) and proliferated ex vivo in response to IL-2 and IL-15 in the absence of antigen (Figure S4J). These memory-like CD44^{hi} CD122$^+$CD8$^+$ cells were remarkably similar to those expanded by pMHC-NPs in NOD mice: FoxP3$^-$CD25$^-$CCR7$^-$CD69$^-$ CXCR3$^+$CD62L^{hi} (Figure 4C and Figures S4L and S4M). Real-time RT-PCR assays for 384 immunological transcripts (Figure S4K) and additional FACS analyses (Figure S4L) highlighted the memory-like phenotype of these T cells, including their expression of granzyme B. Furthermore, like the memory-like CD8$^+$ cells expanded by pMHC-NP, the memory-like CD8$^+$ cells arising in 17.6α-8.3β-TG mice rapidly produced high amounts of IFN-γ, without secreting IL-2 or proliferating, in response to antigen in vitro (Figure 4D and Figure S4N). Thus, by and large, these memory-like low-avidity CD8$^+$ cells are identical in phenotype and function to those that expand in pMHC-NP-treated mice.

Memory CD8$^+$ Cells Arising from Low-Avidity Precursors Have Regulatory Properties

Unlike their CD122$^-$ counterparts or T1D-irrelevant (i.e., LCMV-gp33-specific) CD8$^+$ cells, the CD122$^+$CD8$^+$ cells of 17.6α-8.3β-TG mice inhibited the proliferation of naive CFSE-labeled CD8$^+$ cells from 17.4α-8.3β-TG mice in response to peptide-pulsed DCs (Figure 4E). Suppression was not because of competition for pMHC, because it was not seen when 17.4α-8.3β-CD8$^+$ cells were used both as responders and suppressors (Figure 4E) and because it also occurred in assays employing LCMV-gp33-D^b-specific CD8$^+$ cells as responders (Figure S4O). Furthermore, suppression required a cognate T-APC interaction, because (1) it did not occur when suppressors and responders were activated with CD3 and CD28 mAbs in the absence of APCs (Figure 4E), and (2) it was seen in assays employing DCs pulsed with a range of NRP-A7 concentrations (1–0.01 μM), but not when the DCs were only pulsed with the responder T cells' ligand (gp33) (Figure S4O).

Like the memory-like CD8$^+$ cells of pMHC-NP-treated mice, the memory-like CD8$^+$ cells of 17.6α-8.3β-TG mice blunted the activation of CFSE-labeled 17.4α-8.3β-CD8$^+$ cells in the PLNs of prediabetic NODs (Figure 4F). Furthermore, the CD8$^+$ cells of 17.6α-8.3β-TG mice, but not their CD4$^+$ cells, suppressed the transfer of diabetes by NOD splenic T cells into NOD.*scid* hosts, particularly in those treated with pMHC-NPs (Figures 4G

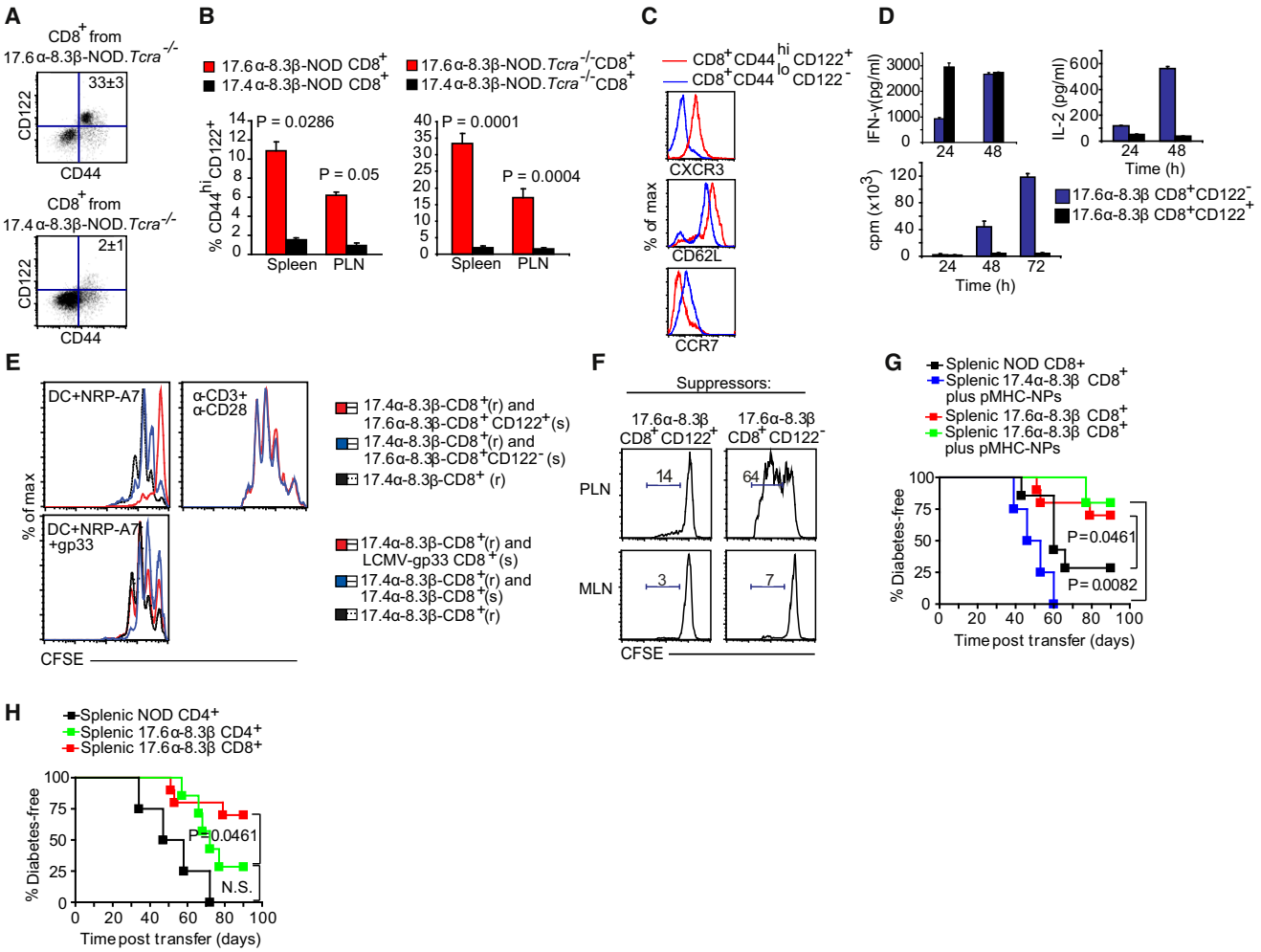

Figure 4. Low-Avidity NRP-V7-K^d-Reactive TCR-TG CD8$^+$ Cells Spontaneously Differentiate into Antidiabetogenic Memory-like T Cells

(A) Representative CD44 versus CD122 profiles of splenic CD8$^+$ cells from 17.6α-8.3β- versus 17.4α-8.3β-NOD.*Tcra*$^{-/-}$ mice.

(B) Percentages of CD44^{hi}CD122$^+$CD8$^+$ cells in spleen and PLN of 17.6α-8.3β-NOD versus 17.4α-8.3β-NOD and 17.6α-8.3β-NOD.*Tcra*$^{-/-}$ versus 17.4α-8.3β-NOD.*Tcra*$^{-/-}$ mice (spleen, n = 4 and 3 and n = 12 and 9, respectively; PLN, n = 4 and 3 and n = 9 and 6, respectively). Mice were 9–18 weeks old.

(C) Phenotypic characteristics. CD8$^+$ cells were stained with CD44, CD122 and CXCR3, CD62L, or CCR7 mAbs.

(D) Secretion of IFN-γ and IL-2, and proliferation in response to NRP-A7-pulsed DCs.

(E) Proliferation of CFSE-labeled 17.4α-8.3β CD8$^+$ cells to NRP-A7- and/or LCMV-gp33-pulsed DCs or CD3 or CD28 mAbs (without APCs) in the presence of naive versus memory CD8$^+$ cells from 17.6α-8.3β-, or naive CD8$^+$ cells from 17.4α-8.3β- or LCMV-gp33-specific TCR-TG-NOD mice. r, responders; s, suppressors.

(F) Proliferation of CFSE-labeled 17.4α-8.3β CD8$^+$ cells in the PLN and MLN of wild-type NOD hosts transfused with CD122$^-$ versus CD122$^+$ 17.6α-8.3β-CD8$^+$ cells.

(G) Splenic CD8$^+$ cells from 17.6α-8.3β-NOD (n = 10), but not NOD, mice (n = 7) suppress the transfer of diabetes by splenic T cells from NOD mice into NOD.*scid* recipients. Other cohorts of hosts were transfused with 17.6α-8.3β-CD8$^+$ cells (n = 5) or 17.4α-8.3β-CD8$^+$ cells (n = 4) and then treated with NRP-V7-K^d-NPs.

(H) Suppression of diabetes cannot be transferred with splenic CD4$^+$ cells of NOD (n = 4) or 17.6α-8.3β-NOD mice (n = 7).

See also Figure S4.

and 4H). In contrast, pMHC-NP-treatment did not afford diabetes protection to hosts transfused with 17.4α-8.3β-CD8$^+$ cells (Figure 4G). Thus, pMHC-NPs potentiate the suppressive activity of autoregulatory T cells but cannot convert a naive autoreactive T cell into a regulatory one.

IFN-γ- and IDO-Dependent Suppression of Antigen Presentation

Addition of blocking mAbs against IL-10 or TGF-β or an adenosine receptor antagonist (8-PST) had no effect on the in vitro suppressive activity of 17.6α-8.3β-CD44^{hi}CD122$^+$CD8$^+$ cells (Figure 5A). In contrast, suppression was abrogated in the presence of an IFN-γ mAb (Figure 5A) or the IDO inhibitor 1-methyl-tryptophan (1-MT). Although necessary, IFN-γ was not sufficient because addition of exogenous IFN-γ to peptide-pulsed APCs did not inhibit their ability to activate 17.4α-8.3β-CD8$^+$ cells. Similar results were obtained when we used NRP-V7-K^d-tetramer$^+$ CD8$^+$ T cells from pMHC-NP-treated NOD mice as suppressors (Figure 5B). Thus, the suppressive activity of autoregulatory CD8$^+$ T cells is IFNγ and IDO dependent.

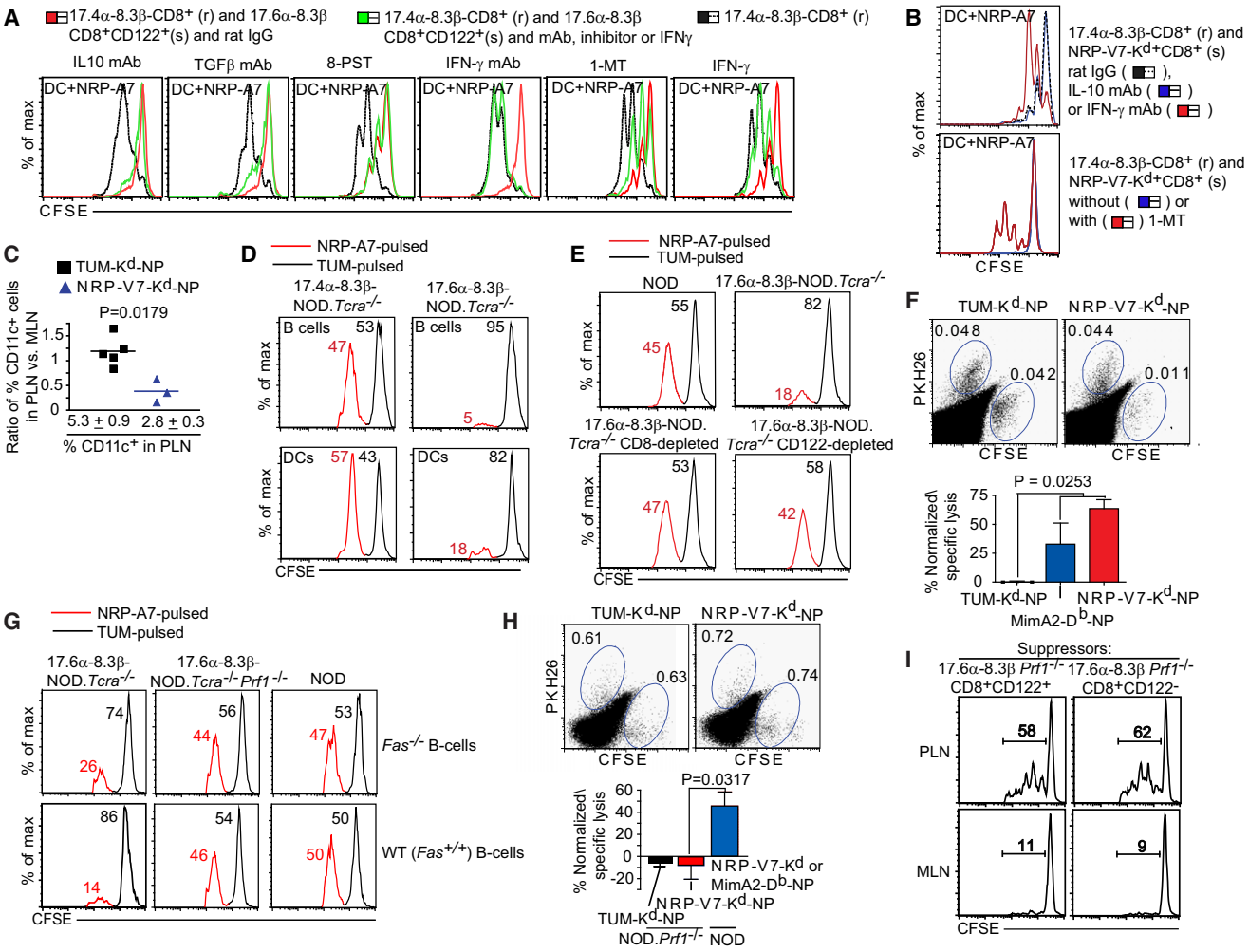

Figure 5. Memory-like Autoregulatory CD8$^+$ Cells Suppress Antigen Presentation via IFNγ- and IDO and Kill Antigen-Pulsed APCs via Perforin

(A) Proliferation of CFSE-labeled 17.4α-8.3β CD8$^+$ cells in response to NRP-A7-pulsed DCs in the absence or presence of memory 17.6α-8.3β-CD8$^+$ cells, rat-IgG, 1-MT, 8-PST, IFN-γ, or blocking mAbs against IL-10, TGFβ, or IFN-γ. r, responders; s, suppressors.

(B) Anti-IFNγ and 1-MT, but not rat-IgG or anti-IL-10, also abrogated the suppressive activity of pMHC-NP-expanded CD8$^+$ cells from NRP-V7-K^d-NP-treated mice.

(C) The PLNs, but not the MLNs, of NRP-V7-K^d-NP-treated mice contain fewer CD11c$^+$ cells than the PLNs from TUM-K^d-NP-treated mice. Data (shown as PLN:MLN ratios) correspond to 15-week-old mice treated with two doses of NP/week for 5 weeks. The average percent of CD11c$^+$ cells in the PLNs of each treatment group are noted below the histograms.

(D) In vivo cytotoxicity assay: NRP-A7- (CFSE^{lo}) or TUM-pulsed (CFSE^{hi}) B cell (upper) or splenic DCs (lower) were injected into TCR-TG hosts (1:1). Survival of transfused APCs in the host spleens was analyzed by FACS 18 hours later.

(E) APC-killing in 17.6α-8.3β-TCR-TG mice is CD8$^+$ and CD122$^+$ T cell-dependent. TUM and NRP-A7-pulsed CFSE-labeled B cells were injected into NOD.*scid* mice that had received non-TG or 17.6α-8.3β splenocytes (unsorted or CD8- or CD122-depleted) 24 hr earlier.

(F) NOD mice treated with NRP-V7-K^d- or MimA2-D^b-NP kill NRP-V7 or MimA2-pulsed DCs in vivo. Top, representative profiles; bottom, mean ± SEM. (n = 3/group). Mice received two weekly doses of NP from the 10th to 15th week. Within 48 hr of the last injection, mice were infused with TUM-pulsed PKH26-labeled or NRP-V7 or MimA2-pulsed CFSE-labeled splenic DCs. DC killing was assessed by comparing the percent of splenic CFSE$^+$ versus PKH26$^+$ cells 18 hr later.

(G) In vivo killing of APCs by 17.6α-8.3β-CD8$^+$CD122$^+$ cells is perforin dependent and Fas independent. CFSE-labeled peptide-pulsed *Fas*$^{+/+}$ or *Fas*$^{-/-}$ B cells were transfused into *Prf1*$^+$ or *Prf1*$^{-/-}$ TCR-TG hosts, and the spleens were analyzed 18 hr later.

(H) In vivo killing of DCs in NRP-V7-K^d-NP-treated mice is perforin-dependent. Experiments were done as in (F). Top panels show representative profiles. Data in bottom panel correspond to TUM-K^d-NP versus NRP-V7-K^d-NP-treated *Prf1*$^{-/-}$ NOD mice (n = 5 mice/group).

(I) Proliferation of CFSE-labeled 17.4α-8.3β CD8$^+$ cells in the PLN and MLN of NOD hosts transfused with CD122$^-$ versus CD122$^+$ CD8$^+$ T cells from *Prf1*$^{-/-}$ 17.6α-8.3β-TCR-TG mice.

See also Figure S5.

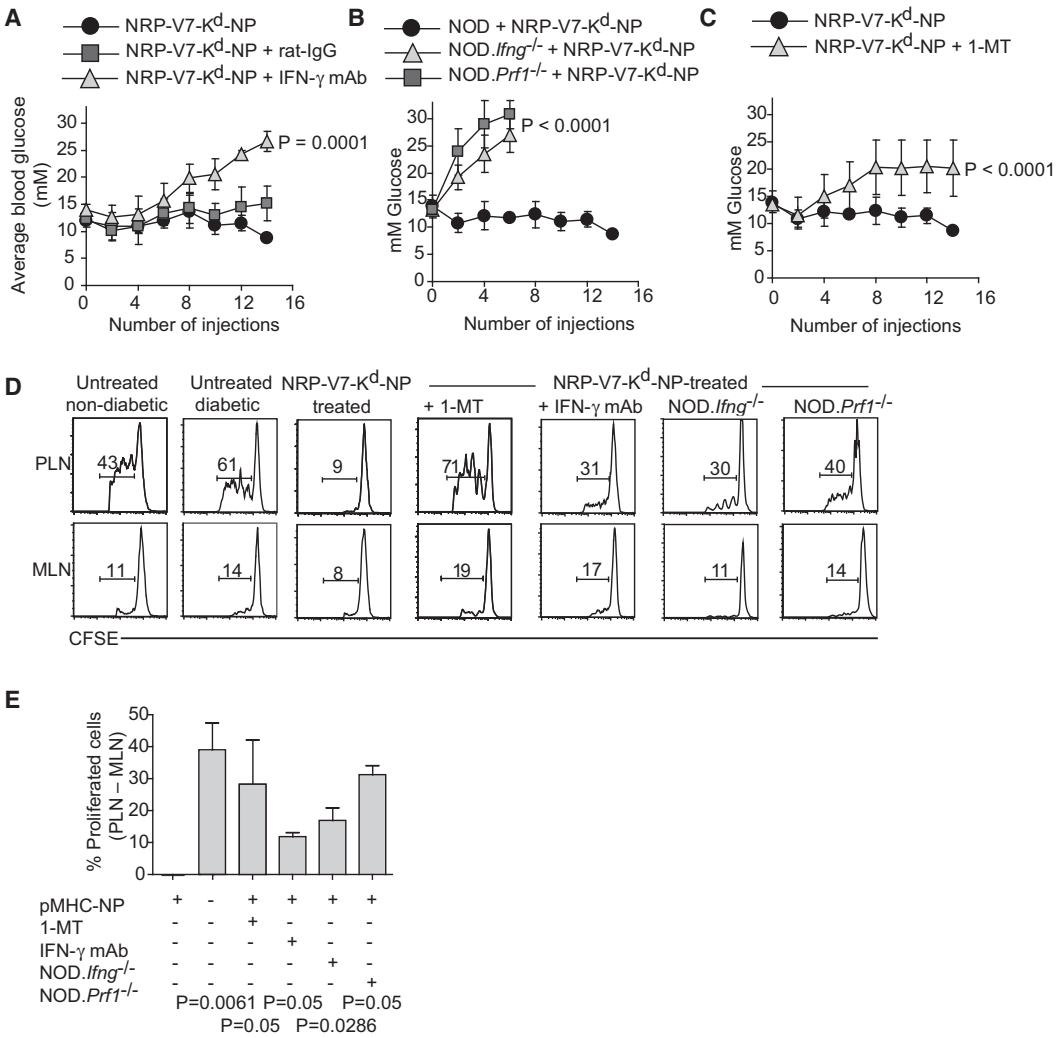

Figure 6. The Anti-T1D Activity of pMHC-NP Also Requires IFN-γ, IDO, and Perforin

(A–C) Average blood glucose levels/group (n = 15 for NRP-V7-K^d-NP; n = 5 for pMHC-NP+rat-IgG; n = 6 for pMHC-NP+IFN-γ mAb; n = 4 for pMHC-NP+1-MT; n = 5 and 8 for pMHC-NP in NOD.*Ifng*$^{-/-}$ and NOD.*Prf1*$^{-/-}$, respectively).

(D and E) Proliferation of CFSE-labeled 17.4α-8.3β-CD8$^+$ cells in the PLN and MLN of untreated nondiabetic or acutely diabetic mice (pooled because there were no differences between the two) and mice from the different groups in (A), except for NOD.*Prf1*$^{-/-}$ hosts, which were 15 weeks old and treated for 5 weeks starting at 10 weeks. (D) shows representative flow profiles and (E) quantitative values. Data correspond to eight untreated (four diabetic), three NRP-V7-K^d-NP-treated, three pMHC-NP+1-MT, three pMHC-NP+IFN-γ mAb, and three each of pMHC-NP-treated NOD.*Ifng*$^{-/-}$ and NOD.*Prf1*$^{-/-}$ mice.

Memory Autoregulatory CD8$^+$ Cells Kill Autoantigen-Bearing APCs via Perforin

A subset of DC-killing memory T cells similar (but not identical) to these CD44^{hi}CD122$^+$CD8$^+$ cells has been described (Guarda et al., 2007). Because IFN-γ was necessary, but not sufficient, for suppression and the memory-like CD8$^+$ cells of 17.6α-8.3β-TG mice expressed granzyme B (Figure S4K), we suspected that suppression might also involve killing of APCs. In fact, the PLNs (but not MLNs) of NRP-V7-K^d-NP-treated mice contained fewer CD11c$^+$ DCs than the PLNs of TUM-K^d-NP-treated controls (Figure 5C).

In vitro, 17.6α-8.3β-CD122$^+$CD8$^+$ cells killed NRP-A7-pulsed NOD DCs, but not islet β-cells, unless they expressed a CD86 transgene, suggesting a role for costimulation in their cytolytic activity (Figure S5A). Furthermore, NRP-A7-pulsed NOD B cells or DCs were rapidly destroyed in diabetes-resistant 17.6α-8.3β-TG hosts but spared in diabetes-prone 17.4α-8.3β-TG mice (Figure 5D and Figure S5B). APC killing was antigen specific (Figure 5D) and was both CD8$^+$ and CD122$^+$ T cell dependent because it could be transferred with bulk, but not CD8- or CD122-depleted, splenocytes (Figure 5E). Similar results were obtained in pMHC-NP-treated NOD hosts: NRP-V7-K^d- and MimA2-D^b-NP-treated (but not untreated) NOD mice specifically eliminated cognate peptide-pulsed DCs in vivo (Figure 5F).

We next asked if APC killing was perforin-dependent. As shown in Figure 5G, whereas perforin (*Prf1*)-competent 17.6α-8.3β-TG mice eliminated both *Fas*$^{-/-}$ and *Fas*$^{+/+}$ NRP-A7-pulsed

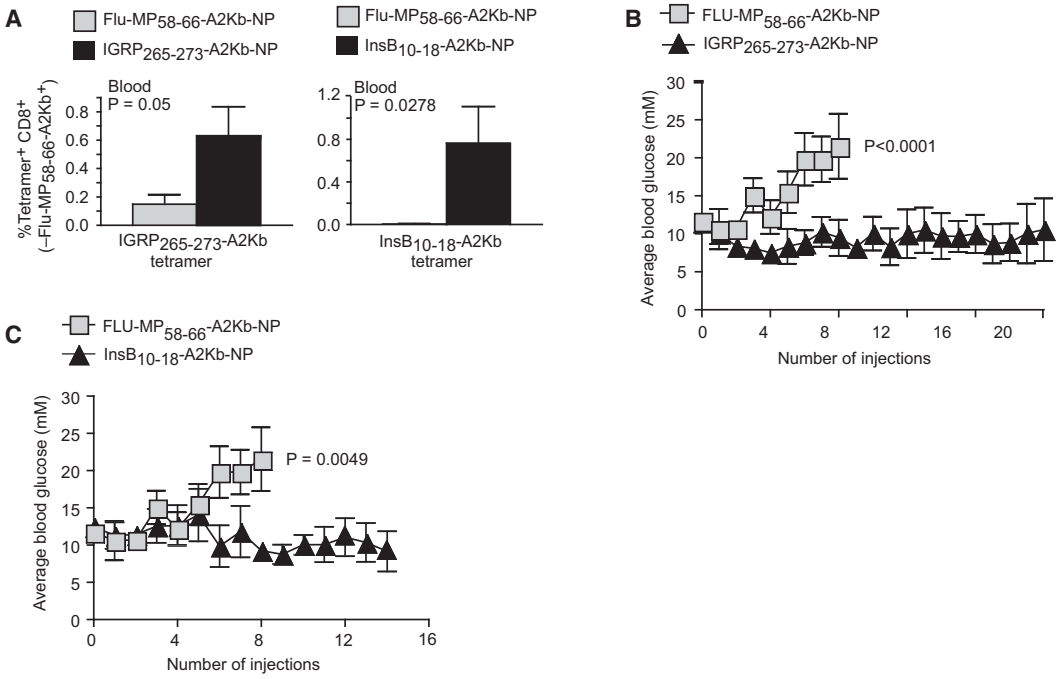

Figure 7. Restoration of Normoglycemia in Diabetic NOD.*HHD* Mice with pHLA-NPs

(A) Average percentages ± SEM of circulating hIGRP$_{265-273}$-A2Kb$^+$ or InsB$_{10-18}$-A2Kb$^+$ CD8$^+$ cells (minus FLU-MP$_{58-66}$-A2Kb$^+$ cells) in hyperglycemic NOD.*HHD* mice treated with FLU-MP$_{58-66}$-A2Kb-, hIGRP$_{265-273}$-A2Kb-, or InsB$_{10-18}$-A2Kb-NPs after ten doses (n = 5, 7, and 5, respectively).

(B and C) Average blood glucose levels in newly diagnosed diabetic NOD.*HHD* mice treated with FLU-MP$_{58-66}$-A2Kb, hIGRP$_{265-273}$-A2Kb, or InsB$_{10-18}$-A2Kb NPs (n = 5, 8, and 7, respectively). Curves include all mice, diabetic and nondiabetic. Mice were euthanized when blood glucose levels were >27 mM.

See also Figure S6.

APCs, their *Prf1*$^{-/-}$ counterparts could not. The memory-like CD8$^+$ cells of these mice also required perforin to suppress autoantigen cross-presentation in the PLNs (Figure 5I versus Figure 4F). Likewise, pMHC-NP-treated, *Prf1*$^{-/-}$ NOD mice failed to eliminate *Fas*$^{+/+}$ NRP-A7-pulsed APCs in vivo (Figure 5H). Thus, memory low-avidity autoregulatory CD8$^+$ cells kill autoantigen-loaded APCs via perforin.

The Anti-T1D Activity of pMHC-NPs Requires IFN-γ, IDO, and Perforin

We then asked if the above mechanisms contributed to pMHC-NP-induced reversal of T1D. We treated newly diabetic NOD mice with NRP-V7-K^d-NPs and rat-IgG (control), IFNγ mAb, or s.c. implants of 1-MT. IFNγ mAb and 1-MT abrogated the therapeutic effect of pMHC-NP (Figures 6A and 6C). Similar results were obtained in diabetic NOD.*Ifng*$^{-/-}$ mice (Figure 6B) that did not respond to pMHC-NP therapy. To investigate the role of APC killing, we screened NOD.*Prf1*$^{-/-}$ mice for hyperglycemia and treated the few mice that developed diabetes with NRP-V7-K^d-NP. Most mice (n = 5/7) remained hyperglycemic (Figure 6B). Furthermore, naive CFSE-labeled 17.4α-8.3β-CD8$^+$ cells proliferated in the PLNs of mice that were refractory to pMHC-NP therapy because of IFNγ blockade or deficiency, IDO inhibition, or *Prf1*-deficiency, but not in the PLNs of wild-type NOD mice treated only with pMHC-NP (Figures 6D and 6E). Thus, pMHC-NP-induced inhibition of autoantigen cross-presentation and T1D require IFNγ, IDO, and perforin.

Effects of NPs Coated with Human T1D-Relevant pHLAs in Humanized NOD Mice

The above results begged the question of whether the pMHC-NP approach might be applicable to human T1D. We focused on two human autoantigenic epitopes that are recognized, with increased frequency, by peripheral blood CD8$^+$ cells of HLA-A2$^+$ diabetic patients (reviewed in Tsai et al., 2008). One spans residues 265–273 of hIGRP (identical to mIGRP$_{265-273}$), and the other spans residues 10–18 of the Insulin B chain.

We first enumerated the presence of these two CD8$^+$ specificities in islets of m*B2m*$^{-/-}$ NOD mice expressing an HLA-A2α1α2-K^{b}α3 transgene covalently linked to hβ2m (NOD.*HHD* mice) using pHLA-A2-Kb tetramers. These mice express HLA-A*0201 in a murine MHC class I-deficient background, exclusively export A*0201-restricted CD8$^+$ cells, and spontaneously develop T1D. Both specificities were found in the islets (and, to a lesser extent, blood) of NOD.*HHD* mice, albeit at significantly different frequencies: ~0.2% mINS$_{10-18}$-A2Kb versus ~0.8% hIGRP$_{265-273}$-A2Kb tetramer$^+$CD8$^+$ cells (using Influenza virus matrix protein (Flu-MP)$_{58-66}$-A2Kb tetramer as negative control [Figure S6A]). Treatment of prediabetic (Figure S6B) or newly diabetic NOD.*HHD* mice (Figure 7A) for 5 weeks with hIGRP$_{265-273}$-A2Kb- or mINS$_{10-18}$-A2Kb-coated NPs caused substantial expansions of the circulating hIGRP$_{265-273}$-A2Kb- or mINS$_{10-18}$-A2Kb-reactive CD8$^+$ cell pools, respectively, compared to Flu-MP$_{58-66}$-A2Kb-NP-treated control mice. Treatment with Flu-MP$_{58-66}$-A2Kb-NPs did not increase the frequency of Flu-MP$_{58-66}$-A2Kb-reactive

$CD8^+$ cells, as expected (data not shown). Importantly, treatment of hyperglycemic NOD.*HHD* mice with $hIGRP_{265-273}$-A2Kb- and $mINS_{10-18}$-A2Kb-NP restored normoglycemia in 7/8 and 5/8 mice, respectively (Figures 7B and 7C and Figures S6D and S6E). In contrast, 4/5 FLU-MP_{58-66}-$A2K^b$-NP-treated mice progressed to frank hyperglycemia (Figures 7B and 7C and Figure S6C). Thus, NPs coated with human T1D-relevant pHLA complexes restore normoglycema in humanized NOD mice. Figure S7 provides a schematic overview of the paradigm on which pMHC-NPs therapy is based.

DISCUSSION

Conventional wisdom based on current knowledge argues that vaccines operating on antigen-experienced lymphocytes would be deleterious in the context of autoimmunity because they would potentiate reactivity against self. Here, we show that lymphocyte memory arising in a chronic organ-specific autoimmune disease (T1D) in response to repeated autoantigen exposure consists largely of pools of low-avidity autoregulatory $CD8^+$ cells. These small pools of disease-driven, antigen-experienced autoregulatory $CD8^+$ cells function as a negative feedback regulatory loop that aims to counter disease progression by inhibiting the activation of naive, pathogenic autoreactive (cognate and noncognate) specificities via suppression of autoantigen-loaded APCs. We further show that suppression of antigen presentation requires engagement of cognate pMHC on the APCs and that it is mediated by at least two different mechanisms: one that involves suppression of function in an IFN-γ- and IDO-dependent manner and another that involves killing of the APC via perforin. Most importantly, we describe a therapeutic approach that exploits this paradigm.

Because high-avidity is usually associated with superior fitness (Oh et al., 2004), it may appear paradoxical that the antigen-experienced $CD44^{hi}CD122^+CD8^+$ cells that mediate pMHC-NP-induced suppression predominantly arise from low-avidity precursors. It should be noted, however, that the autoreactive T cell repertoire, unlike the case for its foreign antigen-specific counterpart, predominantly consists of naive low-avidity T cell clones (Jiang and Chess, 2009). Furthermore, in spontaneous autoimmune diseases, unlike most foreign antigen-specific immune responses, there is chronic autoantigenic persistence. We propose that repeated, low-dose antigenic stimulation of autoreactive T cells induces reactivation-induced cell death of naive and effector high-avidity clones and differentiation of the more prevalent low-avidity autoreactive clones into memory autoregulatory T cells. This scenario is compatible with what we know about effector and memory T cell formation in the context of acute or persistent antigen exposure (Appay et al., 2000; Barber et al., 2006; Lechner et al., 2000; Sprent and Tough, 2001; Williams et al., 2006; Zajac et al., 1998). This hypothesis also accords with the notion that T cells receiving submaximal activation signals are more prone to becoming memory cells than short-lived effectors (Williams et al., 2006). We do not imply that memory T cells only arise from low-avidity precursors. Rather, we suggest that memory T cell generation in chronic autoimmunity occurs more efficiently in the low-avidity T cell pool.

These memory-like autoregulatory $CD8^+$ cells inhibit the presentation of antigens to noncognate T cell specificities in vitro and in vivo in an IFN-γ-, IDO- and perforin-dependent manner. Because IFN-γ can trigger IDO competence and regulatory activity in DCs (Jürgens et al., 2009), IFN-γ may operate, in part, via IDO. Together, these data strongly suggest that these pools of monospecific memory-like T cells that are expanded by pMHC-NP therapy blunt polyclonal autoimmune responses by suppressing the antigen-presenting function of and by directly killing autoantigen-loaded APCs (presenting both cognate and noncognate pMHCs simultaneously). It may seem surprising that these memory-phenotype T cells spare β cells while killing APCs. One possibility, supported by our in vitro data, is that the cytolytic activity of these low-avidity memory autoregulatory $CD8^+$ cells is elicited only when costimulatory molecules are engaged.

Two important characteristics of pMHC-nanovaccines based on this paradigm are noteworthy. The first is that such nanovaccines exclusively expand preexisting (i.e., disease-generated) autoantigen-experienced $CD8^+$ cells and thus would be inconsequential in healthy individuals. The second is that, in principle, they can be engineered with any disease-relevant pMHC complex, regardless of prevalence of the cognate T cell population, provided that it is involved in the disease process. This interpretation stems from two observations: that NPs coated with a pMHC recognized by a prevalent autoreactive $CD8^+$ subset were as effective as those coated with a pMHC recognized by an infrequent subset and that NPs coated with two different human T1D-relevant, but subdominant, pHLA-A2 complexes could restore normoglycemia in NOD.*HHD* mice. It is also worth noting that there is an intriguing parallel between our observations in pMHC-NP-treated mice and the outcome of hOKT3g1 (Ala-Ala) therapy in human T1D patients. These patients have increased percentages of $CD8^+$ cells with in vitro regulatory activity (Bisikirska et al., 2005) and increased percentages of memory-like autoreactive $CD8^+$ cells (Cernea and Herold, 2010). It is conceivable that these T cells correspond to the memory-like autoregulatory $CD8^+$ cells described herein.

In sum, we have shown that progression of T1D results in the generation of pools of antidiabetogenic memory-like autoregulatory $CD8^+$ T cells that can be expanded by systemic delivery of pMHC-NPs. The unique properties of pMHC-coated NPs, coupled with current knowledge of antigenic specificities of autoreactive $CD8^+$ cells in human T1D, make this nanovaccine an attractive candidate for clinical testing. If the paradigm on which this nanovaccine is based held true in other chronic autoimmune diseases involving autoreactive $CD8^+$ cells (Walter and Santamaria, 2005) or is extended to autoregulatory $CD4^+$ T cells, pMHC-nanovaccines might find general applicability in autoimmunity.

EXPERIMENTAL PROCEDURES

Mice

17.6α-8.3β-TG NOD mice were produced by microinjecting TCR$\alpha\beta$ transgenes into NOD zygotes. NOD.*G6pc2*$^{K209A-F213A}$ mice were produced using gene-targeted CK35 ESCs and by backcrossing the targeted allele onto the NOD background. These studies were approved by the institutional animal care committee.

pMHC-NP Synthesis and Therapy

pMHC-coated iron oxide NPs were prepared as described (Moore et al., 2004). Cohorts of 4-week-old female mice were injected i.v. with 0.375–7.5 μg iron in PBS every 2 weeks until the 3rd injection and every 3 weeks thereafter. Cohorts of 10-week-old females were injected with 7.5 μg of NP i.v. twice a week for 5 week . Mice were killed at the onset of T1D or followed for 32 weeks. In other experiments, mice with blood glucose > 11 mM for 2 days were treated i.v. twice a week with pMHC-NP or pMHC tetramers (5 μg) until stably normoglycemic (for 4 weeks) or with CD3 mAb (5 μg) for 5 days. Other cohorts received pMHC-NPs and rat-IgG or IFNγ mAb (500 μg i.p. twice a week for 2 weeks, followed by 200 μg/week for 3 weeks) or implanted s.c. with depots (2 × 175 mg) of 1-MT.

Islet-Associated CD8$^+$ T Cells

Islet-associated CD8$^+$ cells were obtained by culturing islets in 0.5 U/ml Takeda rIL-2 for 6–10 days. CD8$^+$ responses (2 × 10^4) were assayed in cultures with peptide-pulsed (10 μM) splenocytes (10^5) for 48 hr. For TCR repertoire studies, cDNAs from sorted tetramer$^+$ CD8$^+$ cells were amplified with Vα17- and Cα-specific primers, cloned, and sequenced.

Cytokine Secretion and Proliferation

FACS-sorted T cells (2 × 10^4) were incubated with peptide-pulsed (1 μM) DCs (10^4) for 48 hr. The 24 hr supernatants were assayed for IL-2 and IFN-γ. The cells were pulsed with 1 μCi of [^{3}H]-thymidine at 48 hr and harvested 24 hr later. For cytokine-induced proliferation, CFSE-labeled splenic CD8$^+$ cells (2 × 10^4) were incubated with 100 ng/ml rhIL-2 or rmIL-15 for 4 days.

Real-Time RT-PCR

cDNA was amplified using mouse Immunology 384 StellArray qPCR plates with SYBR Green. The data were analyzed using the Global Pattern Recognition analysis tool.

In Vitro Suppression

FACS-sorted CD8$^+$ cells (2 × 10^4) were cultured with gp33- (1 μM) and/or NRP-A7 or V7-pulsed (0.01–1 μM) DCs (10^4) for 24 hr, prior to the addition of CFSE-labeled CD8$^+$ cells (2 × 10^4). In other experiments, sorted CD8$^+$ cells (3 × 10^4) were cocultured with CFSE-labeled 8.3-CD8$^+$ cells (3 × 10^4) in wells coated with CD3 and CD28 mAbs (3 μg/ml). CFSE dilution was measured after 48–72 hr. Sorted tetramer$^+$CD8$^+$ cells from pMHC-NP-treated mice were activated with CD3 mAb (3 μg/ml) + rIL-2 for 72 hr and cultured with peptide-pulsed DCs prior to adding reporter cells. Some cultures received rat-IgG, rat anti-mIL-10, rat anti-mTGFβ, or rat anti-mIFN-γ (all at 10 μg/ml), 8-PST (100 μM), 1-MT (200–400 μM), or IFN-γ (5–20 ng/ml).

In Vivo Suppression of Cross-presentation

Sorted CD122$^+$ and CD122$^-$ CD8$^+$ cells were activated with NRP-A7-pulsed (1 μM) DCs in IL-2 for 3 days. These cells (3.5–7.5 × 10^6) were injected into 8-week-old NOD mice; 24 hr later, the hosts received 15 × 10^6 CFSE-labeled 8.3-CD8$^+$ cells. The PLN and MLN CD8$^+$ cells were examined for CFSE dilution on day 6. In other experiments, we compared proliferation of transfused CFSE-labeled 17.4α-8.3β-CD8$^+$ cells in untreated versus pMHC-NP-treated mice.

In Vivo Cytotoxicity

Purified splenic B cells or DCs were pulsed with peptides (0.01–10 μM) for >2 hr at 37°C. TUM-pulsed cells were labeled with 2 μM PKH26, and NRP-A7, V7, or MimA2-pulsed cells with 0.1 μM CFSE. Alternatively, they were labeled with CFSE (TUM, 3 μM CFSE; NRP-A7, 0.3 μM CFSE) for 3 min at 37°C. After washing, they were mixed 1:1 and injected i.v. (10^7) into TCR-TG- or pMHC-NP-treated mice. The ratios of CFSE$^+$ versus PKH26$^+$ or CFSE^{hi} versus CFSE^{low} B cells or DCs in the host spleen were measured after 18 hr. For in vivo cytotoxicity assays in NOD.*scid* hosts, mice were transfused with 7–10 × 10^7 nondepleted, or CD8- or CD122-depleted splenic cells from 17.6α-8.3β-NOD.*Tcra*$^{-/-}$ mice. Target cells were injected 24 hr later, and survival was assessed after 18 hr.

Transfer of Suppression

Splenic CD8$^+$ or CD4$^+$ cells from 50-week-old nondiabetic untreated mice or pMHC-NP-cured animals (5 × 10^6) or TCR-TG mice (10^7) were transfused i.v. into 5- to 10-week-old NOD.*scid* females. After 24 hr, the hosts received 2 × 10^7 pooled CD4$^+$ and CD8$^+$ splenocytes from 8- to 9-week-old female NOD mice. Diabetes was monitored for 100 days. Some cohorts received cognate pMHC-NPs (i.v., twice/week) after T cell transfer.

Statistical Analyses

Data were compared by Student's t, Mann-Whitney U, Chi-Square, or two-way ANOVA tests.

Additional Experimental Procedures

An expanded version of this section is provided in Supplemental Information.

SUPPLEMENTAL INFORMATION

The Supplemental Information includes seven figures and Supplemental Experimental Procedures and can be found with this article online at doi:10.1016/j.immuni.2010.03.015.

ACKNOWLEDGMENTS

We thank N. Ghyselinck for the pFlEx vector; V. Cerundolo for the A2-Kb construct; D. Serreze for NOD.*Ifng*$^{-/-}$ and NOD.*HHD* mice; S. Bou, M. DeCrom, M. Foote, C. Gwozd, B. Han, T. Irvine, J. Mauricio, H. Metselaar and S. Thiessen for technical assistance; L. Kennedy and L. Robertson for FACS; C. Huang for help with IPGTTs; and L. Edelstein-Keshet, J. Elliott, A. Khadra, Y. Shi, T. Stratmann, and J. Verdaguer for reading the manuscript. This work was supported by the Canadian Institutes of Health Research, the Juvenile Diabetes Research Foundation (JDRF), the Natural Sciences and Engineering Research Council of Canada, and the Canadian Diabetes Association (CDA). S.T., A.S., and P. Serra were supported by Alberta Innovates—Health Solutions, and J.W. is supported by the CDA. P. Santamaria is a Scientist of Alberta Innovates and a JDRF Scholar. The JMDRC is supported by the Diabetes Association (Foothills).

Received: September 24, 2008
Revised: December 18, 2009
Accepted: February 9, 2010
Published online: April 8, 2010

REFERENCES

Aichele, P., Kyburz, D., Ohashi, P.S., Odermatt, B., Zinkernagel, R.M., Hengartner, H., and Pircher, H. (1994). Peptide-induced T-cell tolerance to prevent autoimmune diabetes in a transgenic mouse model. Proc. Natl. Acad. Sci. USA *91*, 444–448.

Amrani, A., Verdaguer, J., Serra, P., Tafuro, S., Tan, R., and Santamaria, P. (2000). Progression of autoimmune diabetes driven by avidity maturation of a T-cell population. Nature *406*, 739–742.

Amrani, A., Serra, P., Yamanouchi, J., Trudeau, J.D., Tan, R., Elliott, J.F., and Santamaria, P. (2001). Expansion of the antigenic repertoire of a single T cell receptor upon T cell activation. J. Immunol. *167*, 655–666.

Anderson, B., Park, B.J., Verdaguer, J., Amrani, A., and Santamaria, P. (1999). Prevalent CD8(+) T cell response against one peptide/MHC complex in autoimmune diabetes. Proc. Natl. Acad. Sci. USA *96*, 9311–9316.

Appay, V., Nixon, D.F., Donahoe, S.M., Gillespie, G.M., Dong, T., King, A., Ogg, G.S., Spiegel, H.M., Conlon, C., Spina, C.A., et al. (2000). HIV-specific CD8(+) T cells produce antiviral cytokines but are impaired in cytolytic function. J. Exp. Med. *192*, 63–75.

Bachmann, M.F., Gallimore, A., Linkert, S., Cerundolo, V., Lanzavecchia, A., Kopf, M., and Viola, A. (1999). Developmental regulation of Lck targeting to the CD8 coreceptor controls signaling in naive and memory T cells. J. Exp. Med. *189*, 1521–1530.

Barber, D.L., Wherry, E.J., Masopust, D., Zhu, B., Allison, J.P., Sharpe, A.H., Freeman, G.J., and Ahmed, R. (2006). Restoring function in exhausted CD8 T cells during chronic viral infection. Nature *439*, 682–687.

Bisikirska, B., Colgan, J., Luban, J., Bluestone, J.A., and Herold, K.C. (2005). TCR stimulation with modified anti-CD3 mAb expands $CD8^+$ T cell population and induces $CD8^+CD25^+$ Tregs. J. Clin. Invest. *115*, 2904–2913.

Cernea, S., and Herold, K.C. (2010). Monitoring of antigen-specific CD8 T cells in patients with type 1 diabetes treated with antiCD3 monoclonal antibodies. Clin. Immunol. *134*, 121–129.

Endharti, A.T., Rifa'I, M., Shi, Z., Fukuoka, Y., Nakahara, Y., Kawamoto, Y., Takeda, K., Isobe, K., and Suzuki, H. (2005). Cutting edge: CD8+CD122+ regulatory T cells produce IL-10 to suppress IFN-gamma production and proliferation of CD8+ T cells. J. Immunol. *175*, 7093–7097.

Guarda, G., Hons, M., Soriano, S.F., Huang, A.Y., Polley, R., Martín-Fontecha, A., Stein, J.V., Germain, R.N., Lanzavecchia, A., and Sallusto, F. (2007). L-selectin-negative CCR7- effector and memory $CD8^+$ T cells enter reactive lymph nodes and kill dendritic cells. Nat. Immunol. *8*, 743–752.

Han, B., Serra, P., Amrani, A., Yamanouchi, J., Marée, A.F., Edelstein-Keshet, L., and Santamaria, P. (2005a). Prevention of diabetes by manipulation of anti-IGRP autoimmunity: high efficiency of a low-affinity peptide. Nat. Med. *11*, 645–652.

Han, B., Serra, P., Yamanouchi, J., Amrani, A., Elliott, J.F., Dickie, P., Dilorenzo, T.P., and Santamaria, P. (2005b). Developmental control of CD8 T cell-avidity maturation in autoimmune diabetes. J. Clin. Invest. *115*, 1879–1887.

Jiang, H., and Chess, L. (2009). How the immune system achieves self-nonself discrimination during adaptive immunity. Adv. Immunol. *102*, 95–133.

Jürgens, B., Hainz, U., Fuchs, D., Felzmann, T., and Heitger, A. (2009). Interferon-gamma-triggered indoleamine 2,3-dioxygenase competence in human monocyte-derived dendritic cells induces regulatory activity in allogeneic T cells. Blood *114*, 3235–3243.

Kaufman, A., and Herold, K.C. (2009). Anti-CD3 mAbs for treatment of type 1 diabetes. Diabetes Metab. Res. Rev. *25*, 302–306.

Lechner, F., Wong, D.K., Dunbar, P.R., Chapman, R., Chung, R.T., Dohrenwend, P., Robbins, G., Phillips, R., Klenerman, P., and Walker, B.D. (2000). Analysis of successful immune responses in persons infected with hepatitis C virus. J. Exp. Med. *191*, 1499–1512.

Lieberman, S.M., and DiLorenzo, T.P. (2003). A comprehensive guide to antibody and T-cell responses in type 1 diabetes. Tissue Antigens *62*, 359–377.

Lieberman, S.M., Evans, A.M., Han, B., Takaki, T., Vinnitskaya, Y., Caldwell, J.A., Serreze, D.V., Shabanowitz, J., Hunt, D.F., Nathenson, S.G., et al. (2003). Identification of the β cell antigen targeted by a prevalent population of pathogenic $CD8^+$ T cells in autoimmune diabetes. Proc. Natl. Acad. Sci. USA *100*, 8384–8388.

Lieberman, S.M., Takaki, T., Han, B., Santamaria, P., Serreze, D.V., and DiLorenzo, T.P. (2004). Individual nonobese diabetic mice exhibit unique patterns of $CD8^+$ T cell reactivity to three islet antigens, including the newly identified widely expressed dystrophia myotonica kinase. J. Immunol. *173*, 6727–6734.

Miller, S.D., Wetzig, R.P., and Claman, H.N. (1979). The induction of cell-mediated immunity and tolerance with protein antigens coupled to syngeneic lymphoid cells. J. Exp. Med. *149*, 758–773.

Moore, A., Grimm, J., Han, B., and Santamaria, P. (2004). Tracking the recruitment of diabetogenic $CD8^+$ T-cells to the pancreas in real time. Diabetes *53*, 1459–1466.

Oh, S., Perera, L.P., Burke, D.S., Waldmann, T.A., and Berzofsky, J.A. (2004). IL-15/IL-15Ralpha-mediated avidity maturation of memory CD8+ T cells. Proc. Natl. Acad. Sci. USA *101*, 15154–15159.

Sallusto, F., Geginat, J., and Lanzavecchia, A. (2004). Central memory and effector memory T cell subsets: function, generation, and maintenance. Annu. Rev. Immunol. *22*, 745–763.

Serreze, D.V., Johnson, E.A., Chapman, H.D., Graser, R.T., Marron, M.P., DiLorenzo, T.P., Silveira, P., Yoshimura, Y., Nathenson, S.G., and Joyce, S. (2001). Autoreactive diabetogenic T-cells in NOD mice can efficiently expand from a greatly reduced precursor pool. Diabetes *50*, 1992–2000.

Sprent, J., and Tough, D.F. (2001). T cell death and memory. Science *293*, 245–248.

Trudeau, J.D., Kelly-Smith, C., Verchere, C.B., Finegood, D.T., Santamaria, P., and Tan, R. (2003). Prediction of spontaneous autoimmune diabetes in NOD mice by quantification of autoreactive T cells in peripheral blood. J. Clin. Invest. *111*, 217–223.

Tsai, S., Shameli, A., and Santamaria, P. (2008). CD8+ T cells in type 1 diabetes. Adv. Immunol. *100*, 79–124.

Verdaguer, J., Yoon, J.W., Anderson, B., Averill, N., Utsugi, T., Park, B.J., and Santamaria, P. (1996). Acceleration of spontaneous diabetes in TCR-β-transgenic nonobese diabetic mice by β-cell cytotoxic CD8+ T cells expressing identical endogenous TCR-α chains. J. Immunol. *157*, 4726–4735.

Verdaguer, J., Schmidt, D., Amrani, A., Anderson, B., Averill, N., and Santamaria, P. (1997). Spontaneous autoimmune diabetes in monoclonal T cell nonobese diabetic mice. J. Exp. Med. *186*, 1663–1676.

Walter, U., and Santamaria, P. (2005). $CD8^+$ T cells in autoimmunity. Curr. Opin. Immunol. *17*, 624–631.

Williams, M.A., Holmes, B.J., Sun, J.C., and Bevan, M.J. (2006). Developing and maintaining protective $CD8^+$ memory T cells. Immunol. Rev. *211*, 146–153.

Zajac, A.J., Blattman, J.N., Murali-Krishna, K., Sourdive, D.J., Suresh, M., Altman, J.D., and Ahmed, R. (1998). Viral immune evasion due to persistence of activated T cells without effector function. J. Exp. Med. *188*, 2205–2213.